ELSEVIER

Volume 180, Number 6, June 2007

JOURNAL OF SOLID STATE CHEMISTRY

www.elsevier.com/locate/jssc

CONTENTS

Abstracted/indexed in BioEngineering Abstracts, Chemical Abstracts, Coal Abstracts, Current Contents/Physics, Chemical, & Earth Sciences, Engineering Index, Research Alert, SCISEARCH, Science Abstracts, and Science Citation Index. Also covered in the abstract and citation database SCOPUS®. Full text available on ScienceDirect®.

Regular Articles

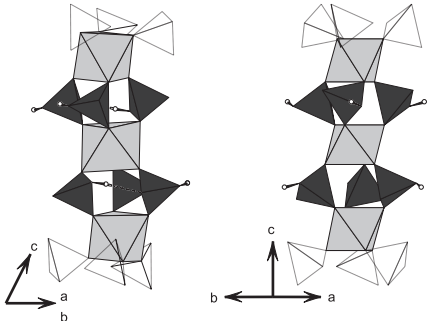

Four new phases in the $AM^{III}(PO_3(OH))_2$ series have been synthesized using hydrothermal techniques. Single crystals XRD studies show that they correspond to two different structural types presenting close relationships. Both three-dimensional host-lattices result indeed from the connection of similar $[M_3(PO_3OH)_6]$ structural units and they present numerous intersecting tunnels containing the monovalent cations. The influence of the size of the A and M cations on the resulting structure type adopted by the compounds of the $AM^{III}(PO_3(OH))_2$ series is examined. The $M_3O_6[PO_3(OH)]_6$ structural basic units encountered in the two studied structure types.

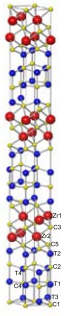

Crystal structure of a new layered carbide, $Zr_2[Al_{3.56}Si_{0.44}]C_5$.

Regular Articles—Continued

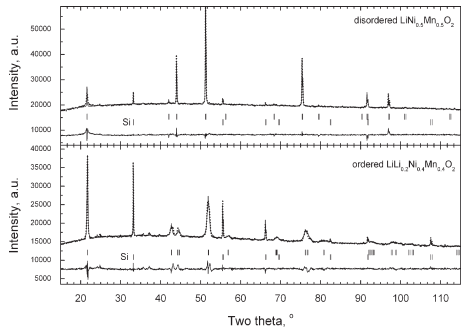

Lithium–nickel–manganese oxides ($Li_{1+x}(Ni_{1/2}Mn_{1/2})_{1-x}O_2$, $x = 0$ and 0.2), having different cationic distributions and an oxidation states of Ni varying from 2+ to 3+, were formed under a high-pressure (3 GPa).

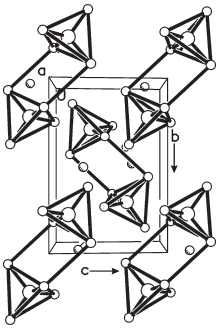

Raman spectroscopy and differential scanning calorimetry are used to monitor the heat and water-stimulated phase transition between the β- and α-anhydrous modifications of $NaHSO_4$. A mechanism for this transition is suggested based on crystallographic considerations of the positions of Na^+ and HSO_4^- in each modification.

A neutron diffraction study of the d^0 and d^{10} lithium garnets $Li_3Nd_3W_2O_{12}$ and $Li_5La_3Sb_2O_{12}$
Edmund J. Cussen and Thomas W.S. Yip
Page 1832

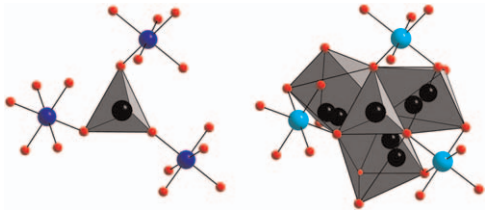

$Li_3Nd_3W_2O_{12}$ contains lithium on a filled tetrahedrally coordinated site. The Li-rich phase $Li_5La_3Sb_2O_{12}$ accommodates lithium on a mixture of tetrahedrally and octahedrally coordinated sites linked by a shared oxide face. The d^0 garnets show substantially contracted unit cells compared to d^{10} analogues.

Superstructure of hollandite $K_xMg_{(8+x)/3}Sb_{(16-x)/3}O_{16}$ ($x \approx 1.76$)
Yuichi Michiue
Page 1840

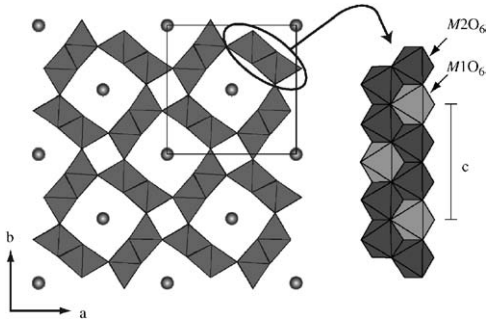

Mg/Sb occupational modulation in a superstructure of hollandite $K_xMg_{(8+x)/3}Sb_{(16-x)/3}O_{16}$ ($x \approx 1.76$) was clarified by the X-ray diffraction technique. The Mg/Sb ratio is 0.8977/0.1023 at the $M1$ site and 0.1612/0.8388 at the $M2$.

Crystal structure of $Ln_{1/3}NbO_3$ (Ln = Nd, Pr) and phase transition in $Nd_{1/3}NbO_3$
Zhaoming Zhang, Christopher J. Howard, Brendan J. Kennedy, Kevin S. Knight and Qingdi Zhou
Page 1846

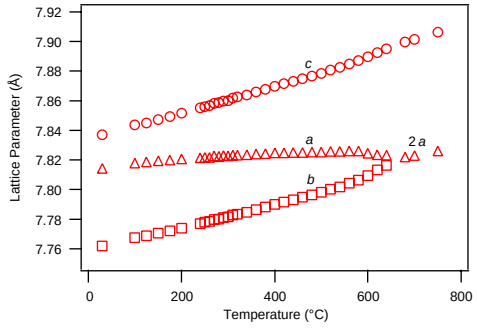

Temperature dependence of the measured lattice parameters through the orthorhombic to tetragonal phase transition in the A-site deficient perovskite $Nd_{1/3}NbO_3$.

Luminescent zinc and cadmium complexes incorporating 1,3,5-benzenetricarboxylate and a protonated kinked organodiimine: From a hydrogen-bonded layer motif to thermally robust two-dimensional coordination polymers
Maxwell A. Braverman, Ronald M. Supkowski and Robert L. LaDuca
Page 1852

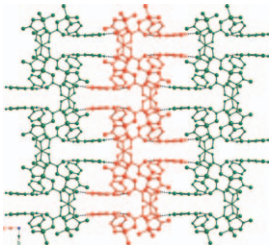

Hydrothermal synthesis has afforded a family of luminescent complexes based on divalent d^{10} cations with 1,3,5-benzenetricarboxylate (BTC) and 4,4′-dipyridylamine (dpa) ligands. $[Zn(HBTC)_2(Hdpa)_2]$ (**1**) is a discrete neutral molecular species. [Zn(BTC)(Hdpa)] (**2**, pictured) and $[Cd(BTC)(H_2O)(Hdpa)]$ (**3**) are 2-D coordination polymers with different morphologies depending on coordination geometry at the metal. All three materials exhibit blue–violet luminescence on exposure to ultraviolet radiation.

Magnesium doping on brownmillerite Ca_2FeAlO_5
J. Malveiro, T. Ramos, L.P. Ferreira, J.C. Waerenborgh, M.R. Nunes, M. Godinho and M.D. Carvalho
Page 1863

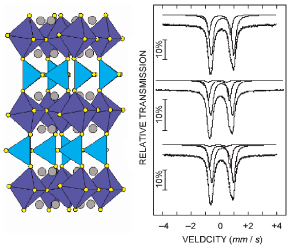

$Ca_2FeAl_{1-x}Mg_xO_5$ ($x = 0$, 0.05, 0.1) compounds with the brownmillerite structure were prepared and characterised. The paramagnetic Mössbauer spectra presented were obtained at $T = 363$ K ($x = 0$); $T = 297$ K ($x = 0.05$) and $T = 353$ K ($x = 0.1$).

Two new hydrogen bond-supported supramolecular compounds assembly from polyoxovanadate and organoamines
Wei-Jie Duan, Xiao-Bing Cui, Yan Xu, Ji-Qing Xu, Hai-Hui Yu, Zhi-Hui Yi, Ji-Wen Cui and Tie-Gang Wang
Page 1875

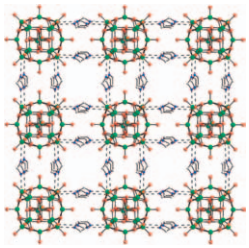

Two new organic–inorganic hybrid compounds based on $[V_{18}O_{42}(PO_4)]$ building blocks have been hydrothermally synthesized. **1** is the first 3-D supramolecular network structure consisting of $[V_{18}O_{42}(PO_4)]$ unit, while **2** possesses 2-D layered supramolecular structure.

Continued

Composition-induced phase transition in $Ca_{14}Zn_{6-x}Ga_{10+x}O_{35+x/2}$ ($x = 0.0$ and 0.5)
S.Ya. Istomin, S.V. Chernov, E.V. Antipov and Yu.A. Dobrovolsky
Page 1882

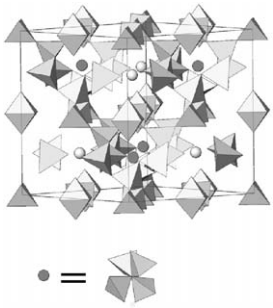

In the crystal structure of $Ca_{14}Zn_6Ga_{10}O_{35}$, only four positions marked by dark circles are occupied by group of four tetrahedra, while four positions marked by light circles are empty. In the crystal structure of $Ca_{14}Zn_{5.5}Ga_{10.5}O_{35.25}$, all eight positions marked by both dark and light circles are randomly occupied by group of four tetrahedra.

Synthesis and crystal structure of $LiBa_2N$ and identification of $LiBa_3N$
Volodymyr Smetana, Volodymyr Babizhetskyy, Grigori V. Vajenine and Arndt Simon
Page 1889

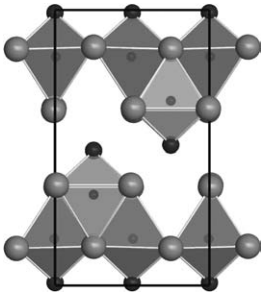

Tetragonal unit cell of $LiBa_2N$.

Order–disorder transition in the complex lithium spinel $Li_2CoTi_3O_8$
Nik Reeves, Denis Pasero and Anthony R. West
Page 1894

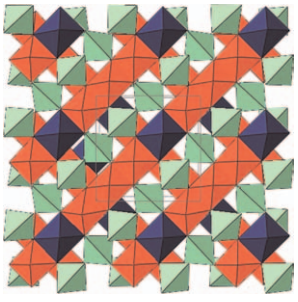

Rietveld refinement of variable temperature neutron powder diffraction data shows an order–disorder phase transition in $Li_2CoTi_3O_8$ commencing at ~500 °C with Li,Co mixing on tetrahedral and octahedral sites. This becomes complete at a first-order structural discontinuity at ~915 °C. Above 930 °C, the structure, space group $Fd\bar{3}m$, has Li, Co and Ti sharing a single-octahedral site and Li, Co sharing a tetrahedral site.

Oxygen non-stoichiometry of $Ln_4Ni_{2.7}Fe_{0.3}O_{10-\delta}$ (Ln = La, Pr)
E.V. Tsipis, M.V. Patrakeev, J.C. Waerenborgh, Y.V. Pivak, A.A. Markov, P. Gaczyński, E.N. Naumovich and V.V. Kharton
Page 1902

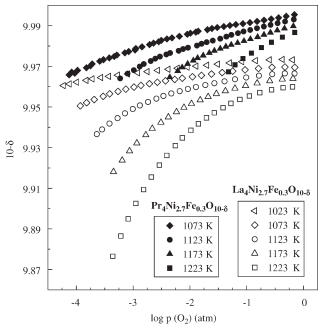

Oxygen deficiency of Ruddlesden-Popper nickelates substituted with iron.

Synthesis, structure of $[H_3dien]\cdot(MF_6)\cdot H_2O$ (M = Cr, Fe) and ^{57}Fe Mössbauer study of $[H_3dien]\cdot(FeF_6)\cdot H_2O$
Amor Ben Ali, Minh Trang Dang, Jean-Marc Grenèche, Annie Hémon-Ribaud, Marc Leblanc and Vincent Maisonneuve
Page 1911

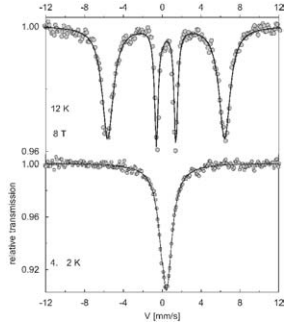

Mössbauer spectra of $[H_3dien]\cdot(FeF_6)\cdot H_2O$.

Effect of the addition of B_2O_3 and $BaO–B_2O_3–SiO_2$ glasses on the microstructure and dielectric properties of giant dielectric constant material $CaCu_3Ti_4O_{12}$
B. Shri Prakash and K.B.R. Varma
Page 1918

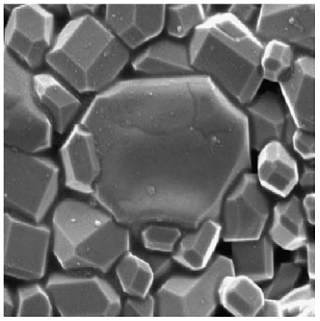

Scanning electron micrograph of 30 wt% BaO–60 wt% B_2O_3–10 wt% SiO_2 (BBS) glass-added $CaCu_3Ti_4O_{12}$ ceramic on sintering.

Highly visible-light luminescence properties of the carboxyl-functionalized short and ultrashort MWNTs

Yongsong Luo, Xiaohong Xia, Ying Liang, Yonggang Zhang, Qinfeng Ren, Jialin Li, Zhijie Jia and Yiwen Tang

Page 1928

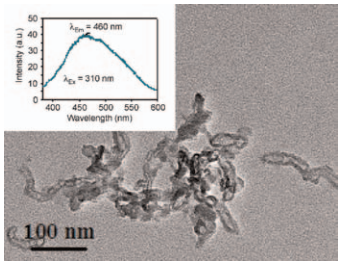

Luminescence of the short and ultrashort multiwalled carbon nanotubes (MWNTs) conjugated with carboxylic acid groups, which is logically attributed to the trapping of excitation energy by defect sites, has been studied.

Structural studies on a high-pressure polymorph of $NaYSi_2O_6$

Volker Kahlenberg, Jürgen Konzett and Reinhard Kaindl

Page 1934

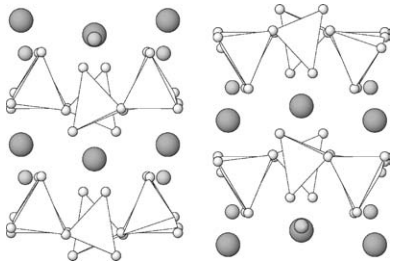

Projection of the whole structure of high-P $NaYSi_2O_6$ parallel to [100].

Synthesis, structure, and properties of the first trimetallic phosphate $[Ni(H_2O)_4]Cd(VO)(PO_4)_2$ with neutral 3-D pillared-layer framework

Shu-Fang Zhang, Guang-Zhen Liu, Shou-Tian Zheng and Guo-Yu Yang

Page 1943

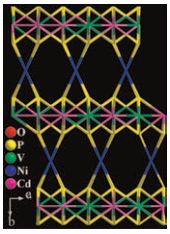

Template-free hydrothermal reactions of $VOSO_4 \cdot 3H_2O$, $CdAc_2 \cdot 2H_2O$, $NiCl_2 \cdot 6H_2O$, H_3PO_4, and H_2O yield the first example of trimetallic phosphate materials, $[Ni(H_2O)_4]Cd(VO)(PO_4)_2$ **1**. Its structure consists of Cd/V/O binary metal oxide lamellas decorated by PO_4 tetrahedra, which are further pillared by $NiO_2(H_2O)_4$ octahedra to generate a neutral 3-D framework containing two intercrossing 8-MR channels.

Rapid Communications

Structural characterizations and magnetic properties of three new reduced molybdenum phosphates

Xiao Zhang, Ji-Qing Xu, Jie-Hui Yu, Jing Lu, Yan Xu, Yan Chen, Tie-Gang Wang, Xiao-Yang Yu, Qing-Feng Yang and Qin Hou

Page 1949

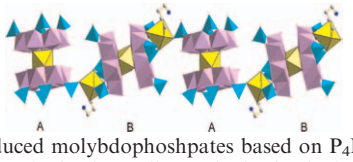

Three new reduced molybdophoshpates based on P_4MO_6 building blocks have been hydrothermally synthesized. **1** is the first covalent 1-D chain consisting of two kinds of forms of $M[P_4MO_6]_2$ units, standing forms A and lying forms B, while **2** and **3** possess 3-D supramolecular network structures. These three compounds all display photoluminescence.